International Immunopharmacology 72 (2019) 264–274

Contents lists available at ScienceDirect

International Immunopharmacology

journal homepage: www.elsevier.com/locate/intimp

Extracellular vesicles derived from bone marrow mesenchymal stem cells attenuate dextran sodium sulfate-induced ulcerative colitis by promoting M2 macrophage polarization

Li Cao[a], Hanxin Xu[b], Ge Wang[a], Mei Liu[a], Dean Tian[a], Zhenglin Yuan[b,*]

[a] Department of Gastroenterology and Hepatology, Tongji Hospital, Tongji Medical College, Huazhong University of Science and Technology, No. 1095 Jiefang Avenue, Wuhan 430030, Hubei, China

[b] Department of Stomatology, Union Hospital, Tongji Medical College, Huazhong University of Science and Technology, No. 1277 Jiefang Avenue, Wuhan 430022, Hubei, China

ARTICLE INFO

Keywords:
Extracellular vesicles
Bone marrow-derived mesenchymal stem cells
Ulcerative colitis
Macrophage polarization
JAK1/STAT1/STAT6 signaling pathway

ABSTRACT

Extracellular vesicles (EVs) secreted by bone marrow mesenchymal stem cells (BMSCs) have shown repairing effects in tissue damage. However, their efficacy and mechanism in the treatment of ulcerative colitis (UC), a type of chronic inflammatory bowel disease, are unclear. To investigate the effects and possible mechanism of EVs in UC treatment, we established an in vitro model using lipopolysaccharide (LPS)-treated macrophages and an in vivo dextran sulfate sodium (DSS)-induced mouse model to mimic UC. In vitro, EVs promoted the proliferation and suppressed inflammatory response in LPS-induced macrophages, as demonstrated by the up-regulation of pro-inflammatory factors (TNF-α, IL-6, and IL-12) and down-regulation of the anti-inflammatory factor IL-10. In the in vivo model, EV administration ameliorated the symptoms of UC by reducing weight loss, disease activity index, and colon mucosa damage and severity while increasing colon length. This was additionally accompanied by the increase in IL-10 and TGF-β levels and the decline in VEGF-A, IFN-γ, IL-12, TNF-α, CCL-24, and CCL-17 levels. In terms of the mechanism, EVs promoted M2-like macrophage polarization, characterized by the increase in the M2 marker CD163. Furthermore, the positive effect of EVs on UC repair seemed to be related to the JAK1/STAT1/STAT6 signaling pathway. Collectively, BMSC-derived EVs exerted positive therapeutic effects against DSS-induced UC, which could be due to a negative inflammatory response.

1. Introduction

Inflammatory bowel disease (IBD), including both Crohn's disease and ulcerative colitis (UC), is a chronic multifactorial disease that affects the gastrointestinal tract and likely results from an aberrant immune response toward luminal antigens in genetically susceptible individuals [1]. UC is clinically manifested by signs such as body weight loss, bloody mucous stool, abdominal pain, rectum atrophy, and easy relapse [2]. The etiology and pathogenesis of UC are believed to be related to genetic susceptibility, immune dysregulation, infection, and environmental factors [3]. Pathophysiological features of UC include the destruction of the epithelial barrier, abnormal immune response induced by the imbalance of intestinal symbiotic flora, immune imbalance between regulatory and effector T cells, and inflammatory cascade induced by leukocyte recruitment [4]. The ultimate manifestations of these characteristics are mucosal inflammation injury and intestinal mucosal imbalance. Clinical trials and treatments of UC mainly focus on anti-inflammatory and mucosal repair and protection, and current treatment of IBD primarily consists of 5-aminosalicylic acid, steroids, antimicrobials, immunomodulators, and monoclonal antibodies [5,6]. However, these medications present limitations, and many patients show no response or become refractory over time. Hence, novel, effective, and safe treatments for UC are urgently needed.

Mesenchymal stem cells (MSCs) are cells that can self-renew and differentiate into various cell types, providing the theoretical basis for the treatment of many diseases [7,8]. Although MSCs can be found in most adult tissues, the primary sources of MSCs for treatment are bone marrow, umbilical cord, and adipose tissues. Among them, bone marrow-derived MSCs (BMSCs) have shown effectiveness in the treatment of chronic diseases, such as knee osteoarthritis [9], type 2 diabetes [10], and UC [11]. In particular, the therapeutic potential of MSCs against UC was demonstrated through MSC transplantation, whereby transforming growth factor-β (TGF-β) signaling was triggered and activated by MSCs to accelerate the recovery of colitis [11].

* Corresponding author.
E-mail address: zldentist@hotmail.com (Z. Yuan).

https://doi.org/10.1016/j.intimp.2019.04.020
Received 20 December 2018; Received in revised form 4 April 2019; Accepted 8 April 2019
Available online 17 April 2019

Extracellular vesicles (EVs) secreted by cells have been described as a new mechanism for cell-cell communication [12]. Various subsets of EVs have been identified, including exosomes (< 150 nm), microvesicles (200–500 nm), and oncosomes (1–10 μm) [13]. When EVs are secreted into the extracellular space in the form of exocytosis, they interact with membrane surface receptors of target cells to regulate signaling pathways and the extracellular environment [14]. EVs can fuse with the target cell membrane to release their contents, including microRNAs, mRNAs, and growth factors, into the cytoplasm and this is believed to be their key physiological function [14]. In turn, the contents of these EVs may exert immunomodulatory effects by triggering cytokine secretion or promoting the expression of inflammatory mediators [15]. MSC-secreted EVs have been used in cell-free therapy to repair tissue damage induced by conditions such as myocardial ischemia/reperfusion [16], autoimmune hepatitis [17], and necrotizing enterocolitis [18]. In addition, EVs from the serum of mice with dextran sodium sulfate (DSS)-induced acute colitis were reportedly involved in macrophage activation, indicating that EVs have potential immunomodulatory effects [19]. However, it remains unknown whether BMSC-derived EVs from can be used in the treatment of DSS-induced UC.

Mononuclear phagocytic cells can differentiate into macrophages of various phenotypes that have different functions under the stimulation of cytokines and microbial products in the cellular microenvironment through a process known as macrophage polarization [20]. M1 macrophages play a vital role in pro-inflammation by inducing type I immune response, killing microbes and tumor cells, and producing a large number of inflammatory factors. Contrarily, M2 macrophages participate in type II immune response by removing residues and promoting angiogenesis [21]. They may also have critical functions in immunoregulation and tissue repair/remodeling by inhibiting the nuclear factor κB and signal transducer and activator of transcription (STAT) signaling pathways [22]. We hypothesized that EVs secreted by BMSCs can inhibit the production of inflammatory factors, promote M1/M2 macrophage polarization in intestinal tissue during UC onset, repair the intestinal mucosa, and delay the occurrence and development of UC.

In this study, we first validated our hypothesis by verifying the effects of BMSC-derived EVs on macrophages in vitro. Then, a DSS-induced UC model was constructed in mice to investigate the protective effect of exogenous EVs on ulcer mucosa repair through macrophage polarization, which may provide a new approach for the treatment of UC.

2. Materials and methods

2.1. Extraction, culture, and identification of mouse peritoneal macrophages

Mouse peritoneal macrophages were extracted as previously described with an improved approach [23]. Two eight-week-old male BALB/c mice were injected with 3.0% thioglycollate medium (1.5 mL/mouse) into the peritoneum to deteriorate it, following a seven-day adaptive feeding period. Three days after injection, the mice were sacrificed and injected with 3 mL of 0.05% ethylenediaminetetraacetic acid/phosphate-buffered saline into the peritoneum to harvest peritoneal macrophages. The collected cells were centrifuged at 200 ×*g* for 5 min at 4 °C, and the cell pellet was washed with phosphate-buffered saline (PBS) and centrifuged again. Then, the cell pellet was suspended in RPMI-1640 medium with 100 U/mL penicillin, 100 μg/mL streptomycin, and 10% fetal bovine serum (FBS). After incubation at 37 °C for 2 h, the cells were washed three times with PBS to remove unattached cells including neutrophils. The cells were cultured at 37 °C in a humidified atmosphere containing 5% CO_2. Macrophages were identified by immunofluorescence staining for CD11b (data not shown) to examine purity and specificity based on a previously reported method [24].

2.2. BMSC isolation and EV extraction

Mouse BMSCs were extracted from an eight-week-old male BALB/c mouse as previously described [25]. Adherent BMSCs were grown in Dulbecco's modified Eagle medium (DMEM) supplemented with 10% FBS until they reached 80% confluence. The cells were trypsinized (0.25% trypsin, Gibco Invitrogen, Carlsbad, CA) for 3 min, followed by neutralization using media containing 10% FBS. Next, the cells were quantified using a hemacytometer, centrifuged at 180 ×*g* for 5 min at 4 °C, and resuspended in sterile PBS at a concentration of 2.0×10^6 cells/mL. For EV extraction from BMSCs, the cells were cultured in serum-free, low-glucose DMEM at 37 °C in a humidified atmosphere of 5% CO_2 for 48 h. Thereafter, the conditioned medium was collected and centrifuged at 1000 ×*g* for 20 min to remove cell debris, followed by centrifugation at 2000 ×*g* for 20 min and 10,000 ×*g* for 20 min. The remaining supernatant was then ultra-centrifuged at 100,000 ×*g* for 70 min to obtain isolated EVs. The purified EVs were collected and stored at −80 °C until use. The samples were imaged using transmission electron microscopy to verify the presence of EVs and the EV surface markers CD63, CD81, and TSG101 were detected by western blot.

2.3. Transmission electron microscopy

To investigate the morphology of the EVs, an EV pellet was placed on a formvar carbon-coated 200-mesh copper electron microscopy grid and incubated for 5 min at room temperature. The grid was then washed with double-steamed water and subjected to standard uranyl acetate staining in the absence of light. The samples were washed once again with double-steamed water and allowed to semi-dry at room temperature before transmission electron microscopic observation (Hitachi HT7700, Tokyo, Japan).

2.4. EV uptake by macrophages

Approximately 20 μg of EVs were collected and labeled according to the instructions of the PKH-67 labeling kit. The PKH67-stained EVs were washed three times using 0.5% PBS to remove excess dye and then co-cultured with 2.0×10^5 macrophages. The cells were visualized after 12 h or 24 h with confocal laser scanning microscopy (Nikon, Tokyo, Japan).

2.5. Treatment of macrophages with lipopolysaccharides (LPS) and EVs

Macrophages were treated with 1 μg/mL LPS [26] for 24 h to construct an in vitro model of UC-induced inflammation. The cell experiments were divided into four groups: Control, LPS treatment, LPS + EVs, and single EV treatment. For the LPS + EVs group, after 30 min of LPS pre-stimulation, macrophages were treated with 100 μg/mL EVs for 24 h. Single EV treatment involved no LPS pre-induction.

2.6. Macrophage phenotype and proliferation

After 24 h, macrophages were collected and labeled with the markers of M1 (interleukin (IL)-12, tumor necrosis factor (TNF)-α, and cluster of differentiation (CD)86) and M2 macrophages (CD163, CD200R, and IL-10). Changes in macrophage phenotype were detected by flow cytometry and the number of cells positive for each marker was statistically analyzed. To verify the effect of EVs on macrophage proliferation, cells were collected at 12 h, 24 h, and 48 h after EV treatment. The absorbance at each time point was measured using Cell Counting Kit-8 (PAB180031, Bioswamp, Wuhan, China) according to the manufacturer's instructions.

2.7. Enzyme-linked immunosorbent assay (ELISA)

To measure the cytokine production levels in the cell culture medium, mouse serum and colon tissue homogenate supernatants were collected and frozen at −80 °C until they were assayed. The levels of tumor necrosis factor-α (TNF-α, MU30030), IL-6 (MU30044), IL-12 (MU30186), and IL-10 (MU30055) in the cell culture medium; vascular endothelial growth factor A (VEGF-A, MU30236), interferon γ (IFNγ, MU30038), IL-12 (MU30186), IL-10, and TNF-α in the serum; and VEGF-A, IL-10, transforming growth factor-β (TGF-β, MU30574), chemokine ligand (CCL)-24 (MU30618), and CCL-17 (MU30804) in colon tissue homogenate supernatants were determined by corresponding ELISA kits (Bioswamp, Wuhan, China) according to the manufacturer's instructions.

2.8. Quantitative reverse-transcription polymerase chain reaction (qRT-PCR)

Total RNA was extracted from frozen macrophage samples or colon tissues using Trizol (15596018, Invitrogen, Carlsbad, CA, USA) and reverse-transcribed into cDNA using the PrimeScript RT Master Mix (RR036Q, TaKaRa Biotechnology, Dalian, China) according to the manufacturer's instructions. qRT-PCR was performed in a 20-μL reaction mixture containing SYBR Green PCR Master Mix (4309155, Applied Biosystems), cDNA, and each primer at 0.2 mmol/L at 95 °C for 10 min, 40 cycles at 95 °C for 10 s, and 60 °C for 45 s. The data was collected using the QuantStudio™ 6 Flex Real-Time PCR System (Applied Biosystems). The relative amount of each gene was normalized to the housekeeping gene GAPDH and analyzed using the $2-\Delta\Delta Ct$ method. Primer sequences are shown in Table 1.

2.9. In vivo UC model and EV treatment

The animal research was approved by the Institutional Animal Care and Use Committee at Tongji Medical College, Huazhong University of Science and Technology (approval number: 2017IACUC795). Thirty specific pathogen-free male BALB/C mice aged 7–8 weeks (weighing 21–23 g) were obtained from the Animal Experiment Center of Huazhong Agricultural University. All mice were maintained under controlled temperature (22 ± 1 °C) and humidity (60 ± 15%) in a 12-h light/dark cycle, given free access to deionized water, fed irradiated disinfectant food, and allowed to acclimatize to the above-mentioned conditions for seven days before experimentation. The mice were randomly divided into three groups (n = 10 per group): control, DSS-induced UC, and DSS-induced UC + EV treatment. To induce UC, the mice were exposed to 3% DSS (42867, Sigma, USA) in the drinking water for seven days. EV treatment was performed via intraperitoneal injection of 50 μg of EVs/mouse/day for seven days [27]. Non-treated mice were injected with the same amount of saline. All mice were sacrificed seven days after treatment to obtain blood and colon tissue samples. The colons were subjected to macroscopic assessment and further processed for microscopic histological evaluation and molecular detection.

Table 1
Primer sequences.

Primer names	Sequences (5′-3′)	Fragment size (bp)
IL-6-F	ACGGCCTTCCCTACTT	126
IL-6-R	TTCCACGATTTCCCAG	
IL-10-F	ACCTGGTAGAAGTGATGC	194
IL-10-R	GACACCTTGGTCTTGGAG	
IL-12-F	TCACGCTACCTCCTCTTT	109
IL-12-R	GGTTTCGGGACTGGCTAA	
TNF-α-F	TCTCATTCCTGCTTGTGG	196
GAPDH-F	CCTTCCGTGTTCCTAC	
GAPDH-R	GACAACCTGGTCCTCA	152

2.10. Daily life records and disease activity index (DAI) evaluation

The body weight, degree of diarrhea, and occult blood or bleeding in the stool of the mice were monitored daily. DAI is a direct indication of the severity of disease symptoms. The DAI was determined by the same technician blinded to the grouping by scoring the extent of body weight loss, stool consistency, stool occult blood positivity, and gross bleeding in accordance with a previously described method [28].

2.11. Macroscopic damage index of mouse colon

After seven days, all mice were sacrificed by cervical dislocation. The colon was removed and measured. The distal colon was excised and cut longitudinally, and the intestinal contents were washed with ice-cold PBS. Macroscopic damage index was assessed blindly by the colon macroscopic scoring system on a 0–4 rating scale with a modified method described as follows: 0, normal mucosa; 1, hyperemia and edema, no ulcers; 2, same as 1 plus small linear ulcers or petechiae; 3, same as 2 plus wide ulcers and necrosis and/or adhesions; 4, same as 3 plus megacolon and/or stenosis and/or perforation.

2.12. Histological assessment of pathological lesions in colon tissues

Formalin-prefixed colon sections were embedded in paraffin and stained with hematoxylin and eosin (H&E) according to standard protocols. Histological microscopic assessment was performed in a blinded fashion by the same pathologist according to a previously described scoring standard [29] to evaluate the severity of inflammation (0, none; 1, mild; 2, moderate; 3, severe), extent of inflammation (0, none; 1, mucosa; 2, mucosa and submucosa; 3, transmural), and crypt damage (0, none; 1, basal one-third damaged; 2, basal two-thirds damaged; 3, crypt lost but surface epithelium present; 4, crypt and surface epithelium lost).

2.13. Myeloperoxidase (MPO) activity assay

MPO activity, an index that indicates the degree of neutrophil infiltration, was measured according to a previously described method [30]. The colon tissue samples were thawed and weighed. Supernatants were obtained from homogenate samples and the MPO activity was determined via a colorimetric method using an MPO assay kit (A044, Nanjing Jiancheng Bioengineering Institute, Nanjing, China) according to the manufacturer's instructions.

2.14. Immunofluorescence staining of macrophage markers

Frozen sections of the distal colon were fixed in freshly prepared 4% paraformaldehyde in PBS and stained for CD86 and CD163, which are markers of M1 and M2 macrophages, respectively. Paraffin-embedded tissue sections were dewaxed, rehydrated, and subjected to antigen retrieval before permeabilization. Thereafter, the colon tissues were blocked with 1% bovine serum albumin (BSA) in PBS for 30 min, incubated overnight with primary antibodies (mouse anti-mouse CD86 and rat anti-mouse CD163) diluted in 1% BSA in PBS at 4 °C, and washed three times with PBS. Then, the samples were incubated with the appropriate secondary antibodies (Alexa Fluor 488 goat anti-mouse IgG or Alexa Fluor 594 goat anti-rat IgG) for 2 h at room temperature. To visualize the cell nuclei, sections were counterstained with 4′,6-diamidino-2-phenylindole for 40 min at 30 °C. The stained sections were examined using a Leica fluorescence microscope.

2.15. Protein extraction and western blot

Total proteins were extracted from EVs or colon tissue using a total

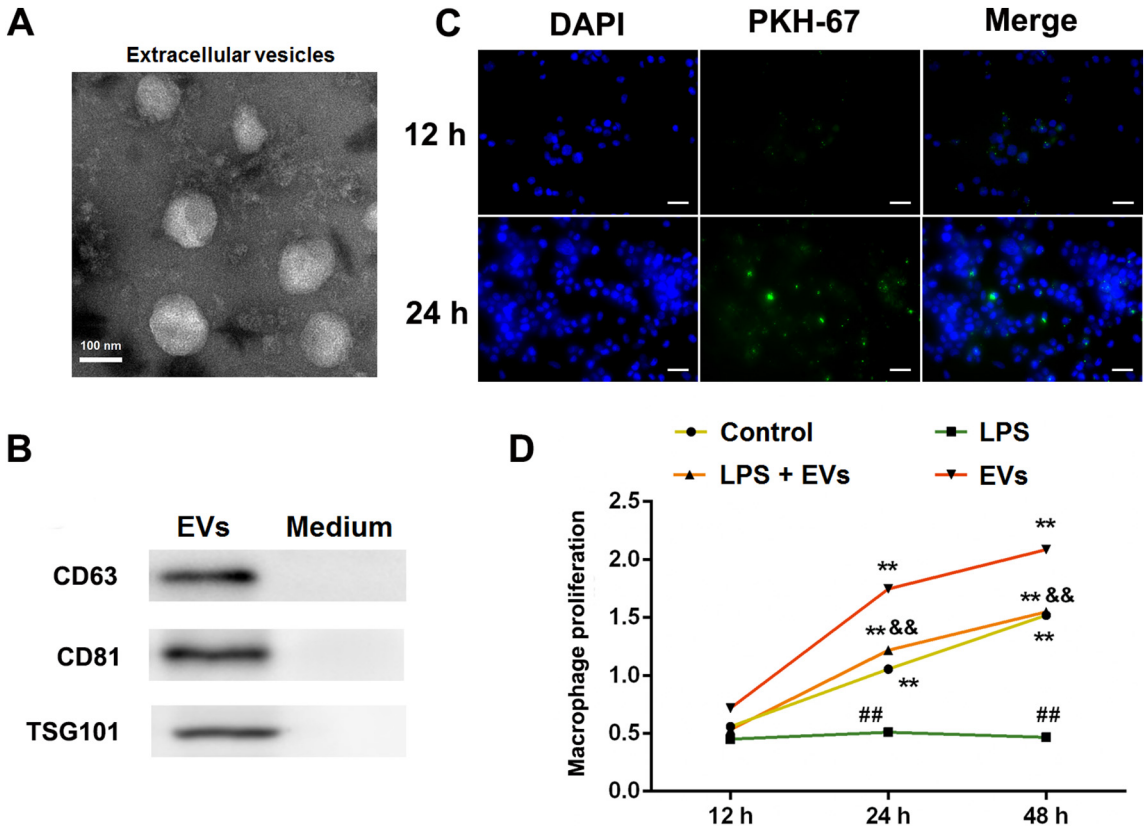

Fig. 1. Identification and characterization of EVs and their effect on macrophage uptake and proliferation. (A) Transmission electron microscopic observation of EVs. Scale bar = 100 nm. (B) Detection of EV markers (CD63, CD81, and TSG101) by western blot. (C) Fluorescence imaging of EV uptake by macrophages at 12 h and 24 h. Scale bar = 50 μm. (D) Macrophage proliferation evaluated by Cell Counting Kit-8. The values are presented as the mean ± SD, n = 3. Compared with the same group at 12 h, $^{**}P < 0.01$; compared with the control at the same time point, $^{\#\#}P < 0.01$; compared with the LPS group at the same time point, $^{\&\&}P < 0.01$.

protein extraction kit (Jiancheng Bioengineering Institute, Nanjing, China) and quantified by the bicinchoninic acid assay. Whole proteins were subjected to 10–15% sodium dodecyl sulfate-polyacrylamide gel electrophoresis and the separated proteins were transferred to polyvinylidene difluoride membranes. Non-specific binding was blocked with 5% skimmed milk for 2 h at 37 °C. Then, the membranes were incubated with rabbit antibodies against CD63 (ab217345, 1:1000, Abcam, Cambridge, UK), CD81 (ab109201, 1:2000, Abcam), TSG101 (ab30871, 1:1000, Abcam), p-Janus kinase 1 (JAK1, ab138005, 1:5000, Abcam), JAK1 (ab133666, 1:5000, Abcam), p-STAT1 (ab30645, 1:1000, Abcam), STAT1 (ab31369, 1:1000, Abcam), p-STAT6 (ab28829, 1:1000, Abcam), and STAT6 (ab44718, 1:200, Abcam) at 4 °C overnight. Next, the membranes were incubated with horseradish peroxidase-conjugated goat anti-rabbit secondary antibody IgG (ab6721, 1:5000, Abcam) for 1 h at room temperature. Images were obtained using the multifunctional Gel Imaging System (Image Quant LAS 500, General Electric, Fairfield, CT, USA) after incubation with enhanced chemiluminescent reagent (P0018A, Shanghai Beyotime Biotechnology Co., Ltd., China).

2.16. Statistical analysis

All experiments were performed in triplicate and values are presented as the mean ± standard deviation (SD). The difference between the two groups was compared with *t*-test. One-way analysis of variance followed by the Tukey's post hoc test was performed to compare differences of multiple groups (> 2) using SPSS 19.0 software (IBM Corp., Armonk, NY, USA). $P < 0.05$ was considered statistically significant.

3. Results

3.1. Macrophages absorbed EVs in a time-dependent manner and EVs promoted proliferation of LPS-treated macrophages

EVs isolated from BMSCs were observed using transmission electron microscopy (Fig. 1A), and their size and specifications were consistent with conventional results. In addition, purified EVs expressed the specific biomarkers CD63, CD81, and TSG101 (Fig. 1B), confirming that EVs have been successfully isolated and identified. To verify the ability of macrophages to absorb EVs, PKH67-labeled EVs were co-cultured with macrophages, and the activity of PKH67-labeled EVs was observed at 12 h and 24 h (Fig. 1C). Over time, the number of EVs absorbed by macrophages gradually increased with a certain degree of time dependence. The effect of EVs on the proliferation of LPS-treated macrophages was subsequently investigated (Fig. 1D). Evidently, LPS treatment inhibited macrophage proliferation, whereas EV treatment alone promoted macrophage proliferation at 24 h and 48 h to a large extent ($P < 0.01$). Furthermore, in LPS-treated macrophages, EV administration promoted proliferation such that it was similar at 24 h and 48 h compared to that of control cells ($P < 0.01$).

3.2. EVs promoted polarization of M1-like macrophages to an M2-like state

The effect of EVs on macrophage polarization was investigated by detecting markers of M1 and M2 macrophages by flow cytometry (Fig. 2). LPS-treated macrophages displayed an increase in the M1 markers CD86, IL-12, and TNF-α ($P < 0.01$, Fig. 2A–C), whereas EVs attenuated the expression of these markers ($P < 0.01$). In terms of M2-like macrophages, compared with the LPS-treated cells, EVs up-regulated the activity of the M2 markers CD163, CD200R, and IL-10

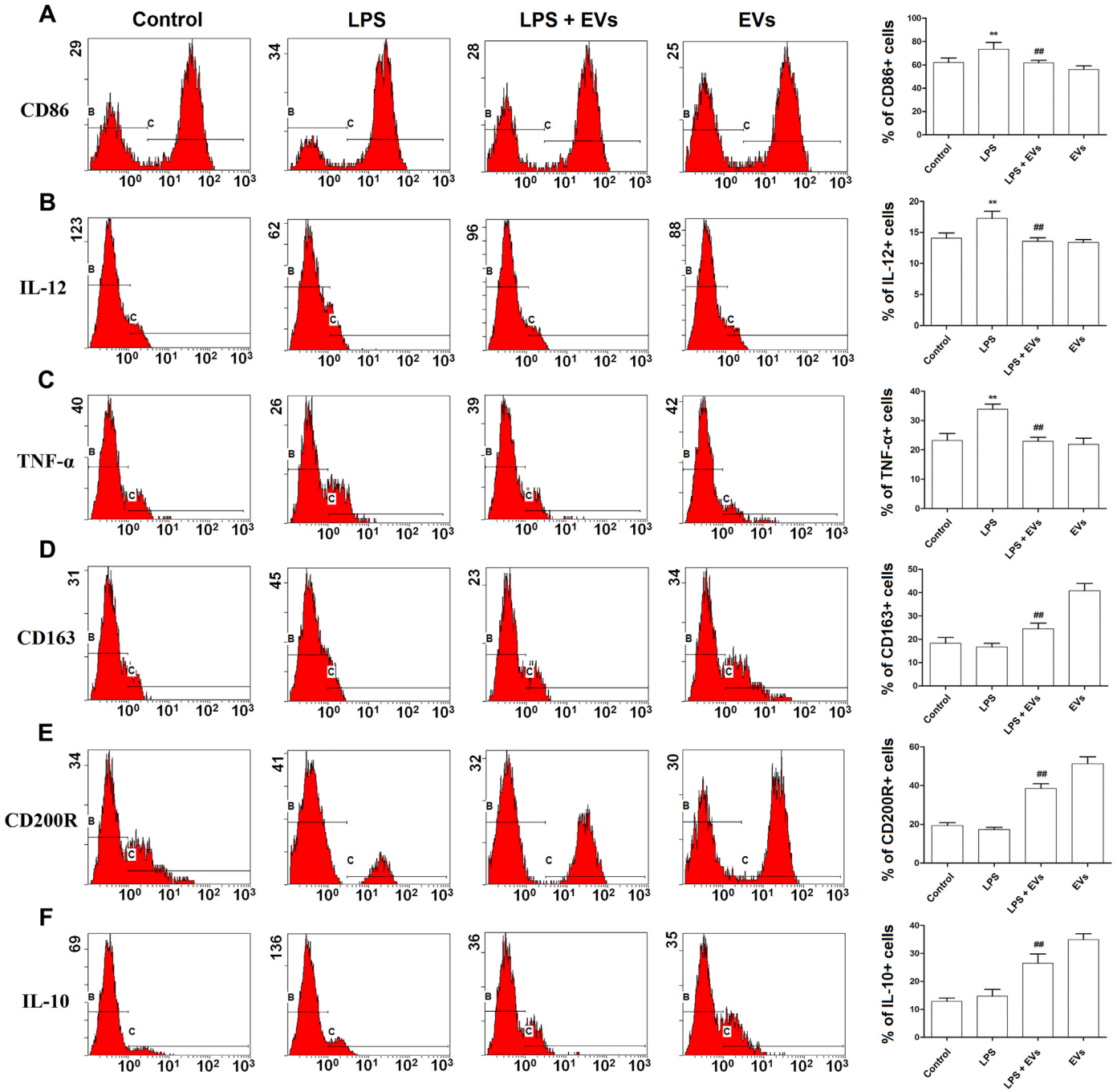

Fig. 2. Evaluation of pro-inflammatory and anti-inflammatory cytokines in macrophages by flow cytometry. Percentage of macrophages positive for M1 markers (A) CD86, (B) IL-12, and (C) TNF-α; and M2 markers (D) CD163, (E) CD200R, and (F) IL-10. The values are presented as the mean ± SD, n = 3. Compared with the control, $^{**}P < 0.01$; compared with the LPS group, $^{\#\#}P < 0.01$.

($P < 0.01$, Fig. 2D–F). Collectively, these results showed that EVs may effectively promote the polarization of M1-like macrophages into an M2-like state.

3.3. EVs suppressed inflammatory response of LPS-treated macrophages

To investigate the effect of EVs on the inflammatory response of LPS-treated macrophages, the activity of inflammatory cytokines was assessed in cell culture supernatants and cultured cells. LPS significantly increased the secretion (Fig. 3A) and mRNA expression (Fig. 3B) of the pro-inflammatory factors TNF-α, IL-6 and IL-12 ($P < 0.01$) in macrophages, whereas the incorporation of EVs attenuated inflammatory response by decreasing the secretion of these factors. By contrast, the secretion and mRNA expression of the anti-inflammatory factor IL-10 were up-regulated by EVs ($P < 0.01$), signifying that EVs may be capable of suppressing LPS-induced inflammatory response.

3.4. EVs attenuated the severity of DSS-induced UC in vivo

In vivo, mice subjected to DSS-induced UC showed significant weight loss ($P < 0.01$, Fig. 4A) and an increase in DAI ($P < 0.01$, Fig. 4B). These effects were reversed by EVs, as reflected by the decline in weight loss percentage and DAI compared to those exhibited by UC-

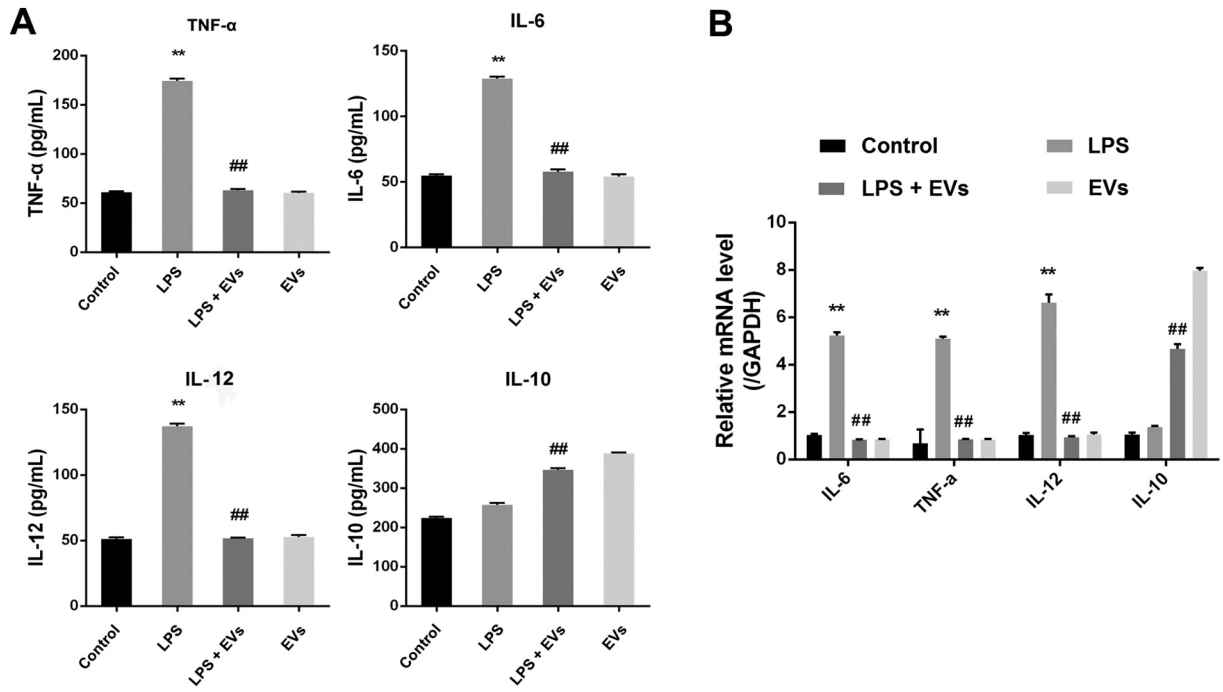

Fig. 3. EVs suppressed inflammatory response in LPS-induced macrophages. (A) Secretion levels of TNF-α, IL-6, IL-12, and IL-10 in cell culture supernatants were evaluated by ELISA. (B) mRNA levels of TNF-α, IL-6, IL-12, and IL-10 extracted from macrophages were evaluated by qRT-PCR. The values are presented as the mean ± SD, n = 3. Compared with the control, $^{**}P < 0.01$; compared with the LPS group, $^{\#\#}P < 0.01$.

induced mice without EV treatment ($P < 0.01$). Next, the gross appearance of the colon was evaluated. As shown in Fig. 4C, EV treatment significantly reversed colon shortening induced by UC. Moreover, no macroscopic damage was observed in the colon tissues from control mice, whereas the intestinal mucosa of UC-induced mice appeared ulcerated, edematous, hyperemic, and hemorrhagic, accompanied by the highest macroscopic colon damage score ($P < 0.01$, Fig. 4D and E). On the contrary, intestinal mucosal injury was alleviated when UC-induced mice were treated with EVs ($P < 0.01$). From a microscopic perspective, the pathological lesions in the colon tissue were evaluated by H&E staining. The colon segments of healthy mice showed a normal structure, whereas severe intestinal mucosal damage was observed in DSS-induced mice, as characterized by increased neutrophils, massive edema, deep infiltration of the superficial mucosal layers, damaged epithelial cells, distorted crypt architecture, and a higher microscopic score than that of the control group ($P < 0.01$, Fig. 4F and G). In turn, colonic lesions in EV-treated mice were reduced to a mild structural damage, accompanied by a lower microscopic score ($P < 0.01$, Fig. 4F and G). On the basis of pathological study, the degree of neutrophil infiltration was evaluated by MPO activity (Fig. 4H). UC-induced colon tissues showed highly increased MPO activity ($P < 0.01$), which was markedly reduced by EV treatment ($P < 0.01$).

3.5. EVs promoted polarization of M1-like macrophages into an M2-like state and reduced inflammatory response in mice with DSS-induced UC

Immunofluorescence was performed to identify the effect of EVs on markers of M1 and M2 macrophages in UC-induced colon tissues (Fig. 5A). In control and UC-induced tissues, prominent staining of the M1 marker CD86 was observed, while the M2 marker CD163 was absent. Upon EV treatment, however, the amount of CD163 increased significantly, as indicated by the bright red staining. Next, ELISA was performed to assess the activity of cytokines and chemokines in the serum and in colon tissues (Fig. 5B and C). UC-induced mice showed an increase in pro-inflammatory factors (VEGF-A, IFN-γ, IL-12, and TNF-α) in the serum and VEGF-A, CCL-24, and CCL-17 in colon tissue homogenate supernatants ($P < 0.01$), but the administration of EVs significantly reduced their levels ($P < 0.01$). In terms of the anti-inflammatory factors IL-10 and TGF-β, EVs further increased their secretion levels ($P < 0.01$). These results showed that EVs exerted a significant anti-inflammatory effect on DSS-induced mice, possibly by promoting the polarization of M1-like macrophages into an M2-like state.

3.6. EVs regulated the JAK1/STAT1/STAT6 signaling pathway in mice with DSS-induced UC

To explore the mechanism of EV function, we examined the activity of JAK/STAT pathway-associated proteins in colon tissues after UC induction and EV administration (Fig. 6A and B). Evidently, the induction of UC via DSS significantly increased the phosphorylation levels of JAK1, STAT1, and STAT6 (normalized to total protein amount) ($P < 0.01$). Down-regulations in JAK1 and STAT1 levels were observed with EV administration ($P < 0.05$ and $P < 0.01$, respectively), accompanied by a remarkable up-regulation in that of STAT6 ($P < 0.01$). These findings show that the anti-inflammatory functions of EVs may be closely related to the regulation of the JAK1/STAT1/STAT6 signaling pathway.

4. Discussion

EVs, which are released by most cell types, are involved in information transmission between cells and soluble factor release. With the recent emergence of cell therapy in medical research, EVs have become a highlight in the treatment of a variety of diseases. In particular, MSC-derived EVs have exerted therapeutic effects on several types of tissue injuries such as myocardial ischemia/reperfusion injury [31] and traumatic brain injury [32]. In this study, we aimed to demonstrate that EVs released by mouse BMSCs ameliorated DSS-induced UC in a mouse model and propose that the underlying mechanisms are mediated by M1/M2 macrophage polarization through JAK1/STAT1/STAT6 signaling.

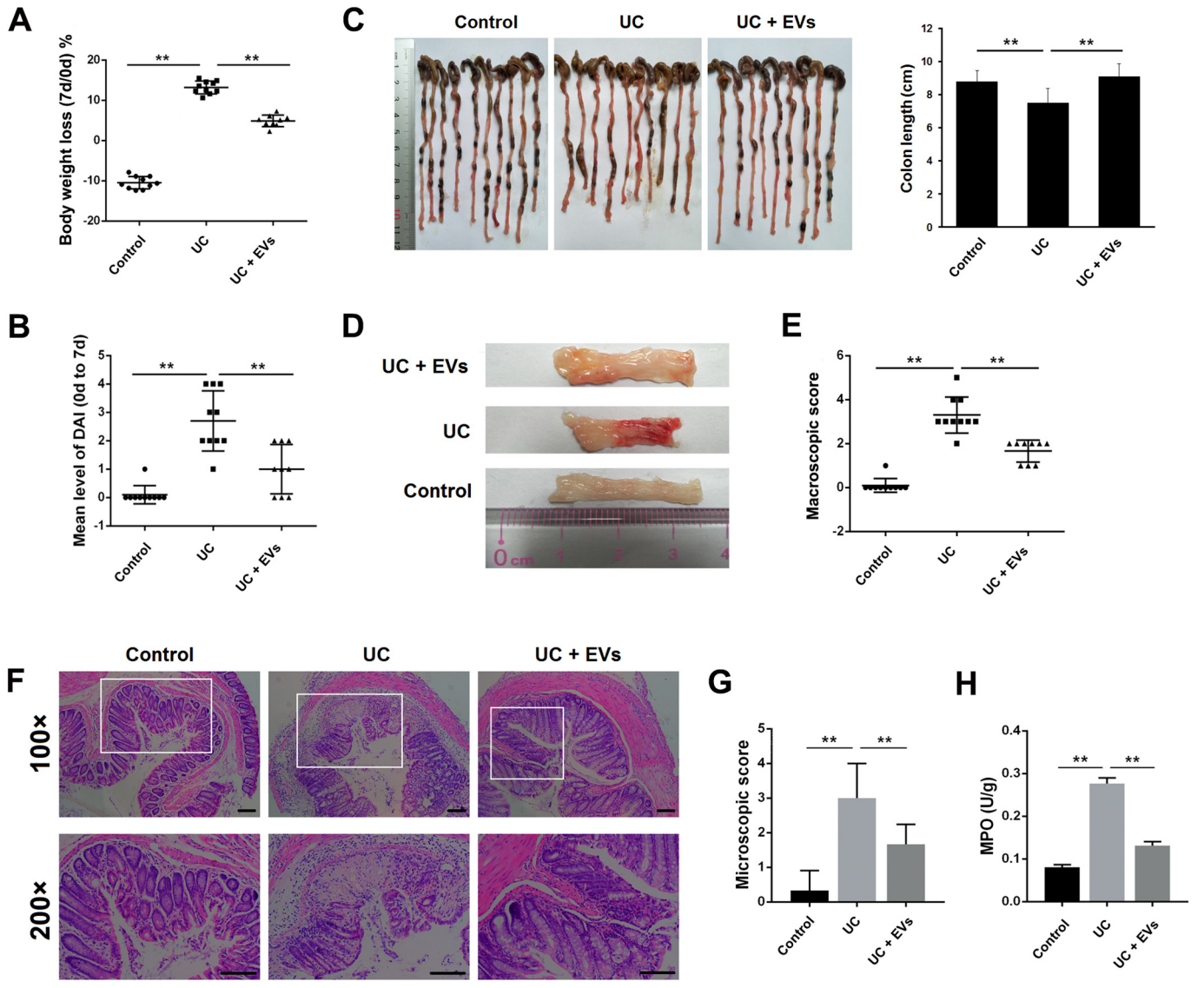

Fig. 4. EVs attenuated the severity of DSS-induced UC in mice at multiple levels. Experiment animals were monitored macroscopically for (A) body weight loss from day 0 to day 7 (%), (B) mean DAI from day 0 to day 7, (C) colon length (photo and quantification), (D) colon damage, and (E) colon damage score. Microscopically, (F) H&E staining of colon tissues (100 × and 200 ×, scale bar = 100 μm), (G) colon injury score, and (H) MPO activity in colon tissues were evaluated. The values are presented as the mean ± SD, n = 3, $^{**}P < 0.01$.

Based on polarization state, macrophages can be identified as either classically activated (M1) or alternatively activated (M2). M1 macrophages are considered pro-inflammatory and cytotoxic because they produce IL-12, TNF-α, and reactive oxygen intermediates [33]. By contrast, M2 macrophages are anti-inflammatory and promote wound healing via TGF-β and IL-10 secretion [34]. We first verified whether EVs regulated macrophage polarization in LPS-treated macrophages. LPS is a common pathogen-associated molecular pattern embedded in the outer membrane of gram-negative bacteria, such as *Escherichia coli* [35]. They are closely associated with toll-like receptor 4 in leukocytes to stimulate the release of pro-inflammatory cytokines and chemokines known to improve bacterial killing and clearance [36]. Macrophage treatment with LPS is an effective in vitro model of UC-induced inflammatory response [35,37]. Our results revealed that BMSC-derived EVs promoted the proliferation of macrophages exposed to LPS (Fig. 1D) and reduced the secretion and expression levels of TNF-α, IL-6, and IL-12, increased IL-10 expression (Fig. 3). The decrease in the expression of M1 markers CD86, IL-12, and TNF-α and the increase in M2 markers CD163, CD200R, and IL-10 (Fig. 2) may be indicative of the M1/M2 polarization of macrophages implicated therein.

The suggestion that EVs play a predominant role in the regulation of macrophage phenotype is supported by relevant studies in the literature. In particular, exosomes (a subset of EVs) derived from LPS-preconditioned MSCs have been shown to exhibit better ability than untreated MSC-derived exosomes to modulate macrophage balance via the up-regulation of anti-inflammatory cytokine expression and promotion of M2 macrophage activation [38]. Moreover, epithelial ovarian cancer-derived exosomes induced M2 polarization by transferring miR-222-3p to macrophages, showing that miRNAs released by EVs may effectively regulate the polarization of tumor-promoting M2 macrophages [39]. Similarly, in a study of experimental bronchopulmonary dysplasia, BMSC-derived exosomes modulated macrophage phenotype, suppressed the pro-inflammatory M1 state, and augmented the anti-inflammatory M2-like state both in vitro and in vivo [40].

Though EVs exhibited evident regulatory effects on macrophage phenotype in vitro, whether and how they affect UC in vivo remain unanswered. To address this question, an in vivo DSS-induced UC model, which is a widely recognized method of investigating the pathological mechanism of IBD [41,42], was established in mice. Consistent with previous studies, we showed that DSS-induced UC resulted

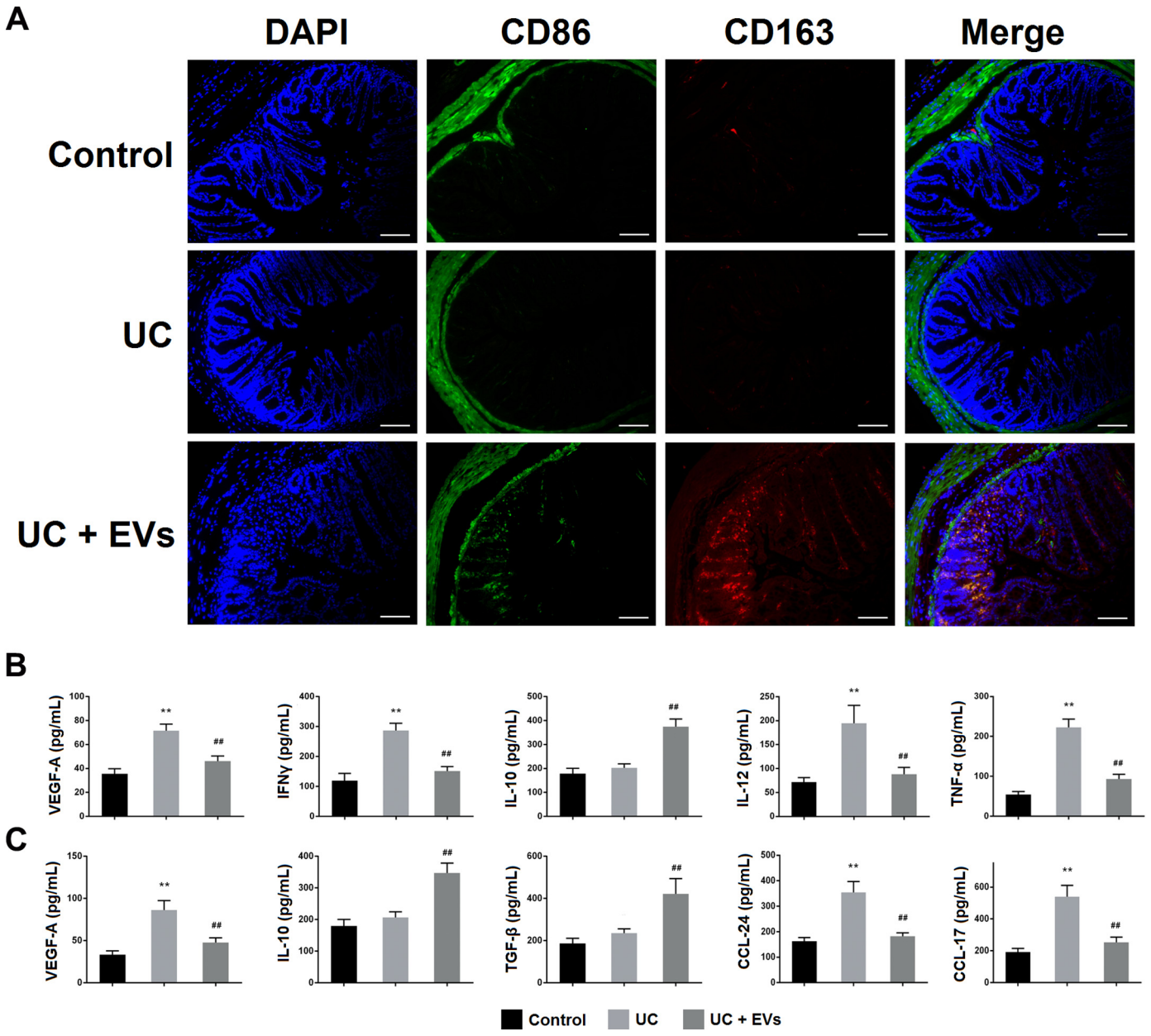

Fig. 5. EVs promoted polarization of M1 macrophages into an M2-like state and reduced the inflammatory response of mice with DSS-induced UC. (A) Detection of M1 (CD86) and M2 (CD163) macrophage markers. Scale bar = 50 μm. ELISA of secretion levels of (B) VEGF-A, IFNγ, IL-10, IL-12, and TNF-α in mouse serum and (C) VEGF-A, IL-10, TGF-β, CCL-24, and CCL-17 in supernatants of mouse colon tissue homogenate. The values are presented as the mean ± SD, n = 3. Compared with the control, $^{**}P < 0.01$; compared with the UC group, $^{\#\#}P < 0.01$.

in body weight loss, elevated DAI score, shorter colons, and increased severity of macroscopic and microscopic colon injury (Fig. 4A–G). In addition, the formation of ulcers in UC-induced mice was accompanied by severe bleeding in the colon and stool. Furthermore, MPO activity, which is a quantitative index of inflammation and a marker of neutrophil infiltration, was markedly elevated in the colon of DSS-treated mice (Fig. 4H). These adverse consequences of DSS-induced UC were alleviated by EVs administration in our animal experiments, as confirmed by the results of microscopic colon evaluation and histopathological observation, collectively exhibiting the anti-inflammatory effect of the EVs used in our study.

UC is a chronic and progressive inflammatory state of the gastrointestinal tract. Colon mucosal lesions are characterized by the infiltration of inflammatory cells, which mainly include macrophages. Macrophages can be stimulated to secrete various types of cytokines and enzymes, further resulting in the injury of intestinal tissue. Normally, M1 and M2 macrophages secrete pro-inflammatory and anti-inflammatory cytokines, respectively [22]. Pro-inflammatory cytokines are a double-edged sword that not only kill pathogenic bacteria but also damage intestinal mucosal cells [43]. The participation of pro-inflammatory cytokines in UC development has been widely demonstrated, and the severity of colitis was reportedly associated with the expression of TNF-α, which is mainly produced in macrophages [44]. Similarly, IFNγ deficiency alleviated colitis by ameliorating stool consistency, rectal bleeding, and colon injury [45], signifying the critical role of IFNγ in inflammation mediation. Furthermore, remarkable up-regulation of VEGF has been found in endoscopic biopsies of UC patients [46]. The regulation of anti-inflammatory cytokines in UC should not be neglected. The mRNA expression of IL-10 was in fact quite low in the bowel tissues of IBD patients [47], whereas TGF-β has been shown

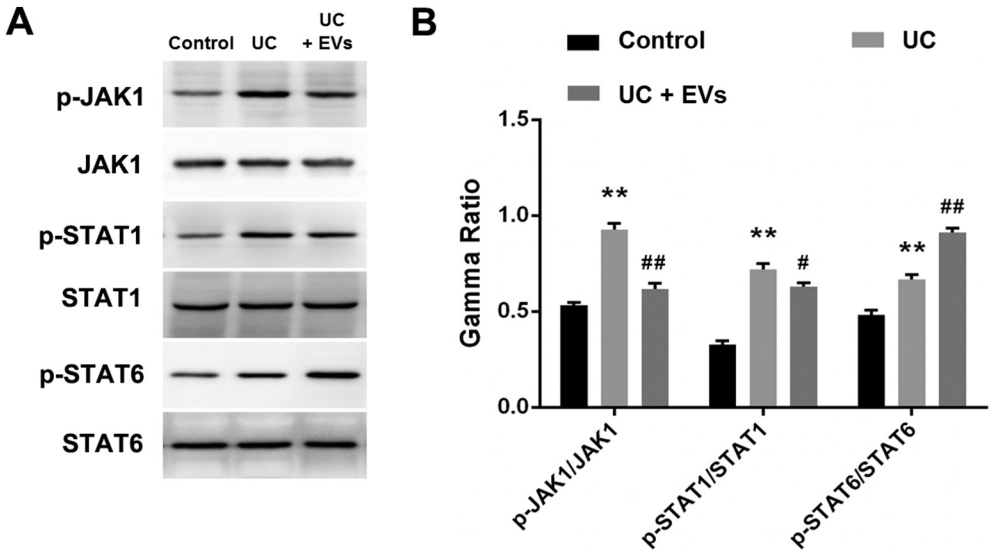

Fig. 6. EVs regulated the JAK1/STAT1/STAT6 signaling pathway in mice with DSS-induced UC. (A) Protein levels of p-JAK1, JAK1, p-STAT1, STAT1, p-STAT6, and STAT6 in mouse colon tissues. (B) Phosphorylation of JAK1 and STAT1 relative to their respective total protein content was significantly decreased by EV treatment after DSS-induced UC, whereas that of STAT6 was significantly decreased. The values are presented as the mean ± SD, n = 3. Compared with the control, $^{**}P < 0.01$; compared with the UC group, $^{\#}P < 0.05$, $^{\#\#}P < 0.01$.

to alleviate DSS-colitis after BMSC transplantation [11]. On this note, IL-10 deficiency in mice led to the development of chronic colitis, but the condition was improved by IL-10 administration, which reduced MPO activity and attenuated TNF-α level [48]. Chemokines are also an essential part of monocyte recruitment during inflammatory response. Specifically, CCL-17 exhibited disease-promoting functions in murine experimental colitis at the histological, cellular, and molecular levels, and the mRNA levels of rectal CCL-11, CCL-24, and CCL-26 were increased in active UC patients [49].

In vivo, EV-treated macrophages showed a decrease in the expression of the M1 marker CD86 and an increase in that of the M2 marker CD163 in colon tissues of mice subjected to DSS-induced UC (Fig. 5A). Correspondingly, EV administration effectively decreased the secretion levels of pro-inflammatory cytokines (VEGF-A, IFNγ, TNF-α, and IL-12) and chemokines (CCL-17 and CCL-24), while those of anti-inflammatory factors (IL-10 and TGF-β) were increased (Fig. 5B and C). These observations may be signs of a shift from an M1-like to an M2-like state in macrophages, but the specific signaling pathways implicated therein require additional in-depth analysis. We therefore investigated the activity of the JAK1/STAT1/STAT6 axis, which has been shown to regulate cytokine signaling and secretion [50,51].

In our study, EVs significantly decreased JAK1 and STAT1 phosphorylation, but increased STAT6 activity (Fig. 6). Members of the JAK and STAT family act in a variety of combinations and when activated, they interact with cytokine receptors to elicit specific cellular responses in complex ways. STAT6 activation via phosphorylation occurs upon JAK1 and JAK3 activation and may indicate pro-inflammatory response in UC [52–54]. Higher levels of STAT6 were observed clinically in the intestinal mucosa of active UC patients compared with those in healthy individuals [53]. However, we showed that EV treatment resulted in an upregulation of p-STAT6 expression in DSS-induced UC, which may be explained by the differential role of STAT6 in the immune system. STAT6 is closely related to IL-4, a cytokine that triggers the alternative activation of macrophages to the M2 state. Importantly, mucosal repair was promoted in murine IBD by M2 macrophage polarization, which was mediated by STAT6-dependent IL-4 signaling [55]. Another member of the STAT family, STAT1, is phosphorylated by the combination of JAK1 with either JAK2 or TYK2. Its involvement of in IFNγ signaling may be evidenced by its elevated levels in the gut tissue of patients suffering from UC and the attenuation of colitis in STAT1-deficient mice [56–58]. It has also been pointed out that JAK1 inhibition exerted anti-inflammatory effects by reversing the disease signature of the colon mucosa in DSS-induced colitis, which was associated with down-regulated STAT3 phosphorylation [59]. Taken together, the pro-inflammatory properties of JAK1, STAT1, and STAT6 are revealed in our study, whereby phosphorylation of all three factors was evident after UC induction. EV treatment attenuated the expression of p-JAK1 and p-STAT1, which is indicative of anti-inflammatory response and corresponds to the previously presented results on the up-regulation of anti-inflammatory cytokines. Contrarily, the up-regulation of p-STAT6 can be clarified by the IL-4-mediated M2 polarization of macrophages, as discussed above. This observation supports our argument of M1/M2 polarization via EV administration, ultimately validating the claims of our hypothesis.

5. Conclusion

Collectively, our findings suggest that EVs derived from mouse BMSCs promoted M2-like macrophage polarization and relieved inflammatory responses, in turn attenuating DSS-induced UC. This process is potentially mediated by the JAK1/STAT1/STAT6 signaling pathway. The use of mouse BMSCs-derived EVs may provide a novel approach for the treatment of UC via regulating inflammatory properties and macrophage phenotype.

Conflict of interest

The authors declare that there is no conflict of interest.

Funding

This work was supported by the Natural Science Foundation of Hubei Province project no. 2017CFB243.

Author contributions

L. C. and Z. Y. conceptualized and designed the study. G. W. performed the in vitro experiments. C. L., H. X., and G. W. were involved in the establishment of the in vivo model and all animal experiments. L. C. wrote the manuscript. M. L., D. T., and Z. Y. assisted in the writing and revision of the manuscript.

References

[1] B. Khor, A. Gardet, R.J. Xavier, Genetics and pathogenesis of inflammatory bowel disease, Nature 474 (7351) (2011) 307–317.
[2] H. Matsuoka, H. Ikeuchi, M. Uchino, T. Bando, Y. Takesue, T. Nishigami, et al., Clinicopathological features of ulcerative colitis-associated colorectal cancer pointing to efficiency of surveillance colonoscopy in a large retrospective Japanese

cohort, Int. J. Color. Dis. 28 (6) (2013) 829–834.
[3] R.B. Sartor, Mechanisms of disease: pathogenesis of Crohn's disease and ulcerative colitis, Nat Clin Pract Gastroenterol Hepatol 3 (7) (2006) 390–407.
[4] M.H. Holtmann, P.R. Galle, Current concept of pathophysiological understanding and natural course of ulcerative colitis, Langenbeck's Arch. Surg. 389 (5) (2004) 341–349.
[5] B.G. Feagan, P. Rutgeerts, B.E. Sands, S. Hanauer, J.-F. Colombel, W.J. Sandborn, et al., Vedolizumab as induction and maintenance therapy for ulcerative colitis, N. Engl. J. Med. 369 (8) (2013) 699–710.
[6] T. Ohkusa, K. Kato, S. Terao, T. Chiba, K. Mabe, K. Murakami, et al., Newly developed antibiotic combination therapy for ulcerative colitis: a double-blind placebo-controlled multicenter trial, Am. J. Gastroenterol. 105 (8) (2010) 1820–1829 [Internet]. Available from https://doi.org/10.1038/ajg.2010.84.
[7] F.H. Chen, R.S. Tuan, Mesenchymal stem cells in arthritic diseases, Arthritis Res Ther. 10 (5) (2008) 1–12.
[8] A. Uccelli, L. Moretta, V. P. Mesenchymal stem cells in health and disease, Nat Rev Immunol 8 (9) (2008) 726–736.
[9] A. Vega, M.A. Martín-Ferrero, Canto F. Del, M. Alberca, V. García, A. Munar, et al., Treatment of knee osteoarthritis with allogeneic bone marrow mesenchymal stem cells: a randomized controlled trial, Transplantation 99 (8) (2015) 1681–1690.
[10] R. Jiang, Z. Han, G. Zhuo, X. Qu, X. Li, X. Wang, et al., Transplantation of placenta-derived mesenchymal stem cells in type 2 diabetes: a pilot study, Front Med China 5 (1) (2011) 94–100.
[11] C. Wang, J. Chen, L. Sun, Y. Liu, TGF-beta signaling-dependent alleviation of dextran sulfate sodium-induced colitis by mesenchymal stem cell transplantation, Mol. Biol. Rep. 41 (8) (2014) 4977–4983.
[12] G. Turturici, R. Tinnirello, G. Sconzo, F. Geraci, Extracellular membrane vesicles as a mechanism of cell-to-cell communication: advantages and disadvantages, Am J Physiol Physiol. 306 (7) (2014) C621–C633.
[13] S.L.N. Maas, X.O. Breakefield, A.M. Weaver, Extracellular vesicles: unique intercellular delivery vehicles, Trends Cell Biol. 27 (3) (2017) 172–188.
[14] I. Prada, J. Meldolesi, Binding and fusion of extracellular vesicles to the plasma membrane of their cell targets, Int. J. Mol. Sci. 17 (8) (2016).
[15] P. Altevogt, N.P. Bretz, J. Ridinger, J. Utikal, V. Umansky, Novel insights into exosome-induced, tumor-associated inflammation and immunomodulation, Semin. Cancer Biol. 28 (2014) 51–57 [Internet]. Available from https://doi.org/10.1016/j.semcancer.2014.04.008.
[16] R.C. Lai, F. Arslan, M.M. Lee, N.S.K. Sze, A. Choo, T.S. Chen, et al., Exosome secreted by MSC reduces myocardial ischemia/reperfusion injury, Stem Cell Res [Internet] 4 (3) (2010) 214–222. Available from: https://doi.org/10.1016/j.scr.2009.12.003.
[17] L. Chen, Lu F bin, Chen D. zhi, Wu J lu, Hu E de, Xu L man, et al., BMSCs-derived miR-223-containing exosomes contribute to liver protection in experimental autoimmune hepatitis, Mol. Immunol. 93 (November 2017) (2018) 38–46.
[18] T.M. Rager, J.K. Olson, Y. Zhou, Y. Wang, G.E. Besner, Exosomes secreted from bone marrow-derived mesenchymal stem cells protect the intestines from experimental necrotizing enterocolitis, J Pediatr Surg [Internet] 51 (6) (2016) 942–947. Available from: https://doi.org/10.1016/j.jpedsurg.2016.02.061.
[19] W.Y. Wong, M.M.L. Lee, B.D. Chan, R.K.T. Kam, G. Zhang, A.P. Lu, et al., Proteomic profiling of dextran sulfate sodium induced acute ulcerative colitis mice serum exosomes and their immunomodulatory impact on macrophages, Proteomics 16 (7) (2016) 1131–1145.
[20] H. He, J. Xu, C.M. Warren, D. Duan, X. Li, L. Wu, et al., Endothelial cells provide an instructive niche for the differentiation and functional polarization of M2-like macrophages, Blood 120 (15) (2012) 3152–3162.
[21] A. Shapouri-Moghaddam, S. Mohammadian, H. Vazini, M. Taghadosi, S.-A. Esmaeili, F. Mardani, et al., Macrophage plasticity, polarization, and function in health and disease, J. Cell. Physiol. 233 (2018) 6425–6440.
[22] P.J. Murray, Macrophage polarization, Annu. Rev. Physiol. 79 (1) (2017) 541–566 [Internet]. Available from http://www.annualreviews.org/doi/10.1146/annurev-physiol-022516-034339.
[23] A. Aronis, M. Aharoni-Simon, Z. Madar, O. Tirosh, Triacylglycerol-induced impairment in mitochondrial biogenesis and function in J774.2 and mouse peritoneal macrophage foam cells, Arch. Biochem. Biophys. 492 (1–2) (2009) 74–81 [Internet]. Available from https://doi.org/10.1016/j.abb.2009.09.011.
[24] B. Wan, J.T. Fleming, T.W. Schultz, G.S. Sayler, In vitro immune toxicity of depleted uranium: effects on murine macrophages, CD4+ cells, and gene expression profiles, Environ. Health Perspect. 114 (1) (2006) 85–91.
[25] P. Tropel, D. Noël, N. Platet, P. Legrand, A.L. Benabid, F. Berger, Isolation and characterisation of mesenchymal stem cells from adult mouse bone marrow, Exp. Cell Res. 295 (2) (2004) 395–406.
[26] S.L. Weinstein, M.R. Gold, A.L. Defrancot, Bacterial lipopolysaccharide stimulates protein tyrosine phosphorylation in macrophages, Proc. Natl. Acad. Sci. U. S. A. 88 (1991) 4148–4152.
[27] L. Wang, Z. Yu, S. Wan, F. Wu, W. Chen, B. Zhang, et al., Exosomes derived from dendritic cells treated with Schistosoma japonicum soluble egg antigen attenuate DSS-induced colitis, Front. Pharmacol. 8 (September) (2017) 1–10.
[28] S.N.S. Murthy, H.S. Cooper, H. Shim, R.S. Shah, S.A. Ibrahim, D.J. Sedergran, Treatment of dextran sulfate sodium-induced murine colitis by intracolonic cyclosporin, Dig. Dis. Sci. 38 (9) (1993) 1722–1734.
[29] L.A. Dieleman, M.J.H.J. Palmen, H. Akol, E. Bloemena, A.S. Pena, S.G.M. Meuwissen, Chronic experimental colitis induced by dextran sulphate sodium (DSS) is characterized by Th1 and Th2 cytokines, Clin. Exp. Immunol. 114 (3) (1998) 385–391 [Internet]. Available from: http://www.ncbi.nlm.nih.gov/entrez/query.fcgi?db=pubmed&cmd=Retrieve&dopt=AbstractPlus&list_uids=9844047.
[30] L.X. Sang, B. Chang, C. Dai, N. Gao, W.X. Liu, M. Jiang, Heat-killed VSL#3 ameliorates dextran sulfate sodium (DSS)-induced acute experimental colitis in rats, Int. J. Mol. Sci. 15 (1) (2013) 15–28.
[31] H. Haga, I.K. Yan, D. Borelli, A. Matsuda, M. Parasramka, N. Shukla, et al., Extracellular vesicles from bone marrow derived mesenchymal stem cells protect against murine hepatic ischemia-reperfusion injury, Liver Transpl. 23 (6) (2018) 791–803.
[32] Y. Yang, Y. Ye, X. Su, J. He, W. Bai, X. He, MSCs-derived exosomes and neuroinflammation, neurogenesis and therapy of traumatic brain injury, Front Cell Neurosci [Internet] 11 (February) (2017) 1–12. Available from: http://journal.frontiersin.org/article/10.3389/fncel.2017.00055/full.
[33] G.A. Duque, A. Descoteaux, Macrophage cytokines: involvement in immunity and infectious diseases, Front. Immunol. 5 (2014) 1–12.
[34] P. Italiani, D. Boraschi, From monocytes to M1/M2 macrophages: phenotypical vs. functional differentiation, Front. Immunol. 5 (OCT) (2014) 1–23.
[35] Y. Kono, S. Miyoshi, T. Fujita, Dextran sodium sulfate alters cytokine production in macrophages in vitro, Pharmazie 71 (2016) 619–624.
[36] Y.C. Lu, W.C. Yeh, P.S. Ohashi, LPS/TLR4 signal transduction pathway, Cytokine 42 (2) (2008) 145–151.
[37] J. Hambleton, S.L. Weinstein, L. Lem, A.L. DeFranco, Activation of c-Jun N-terminal kinase in bacterial lipopolysaccharide-stimulated macrophages, Proc. Natl. Acad. Sci. U. S. A. 93 (1996) 2774–2778.
[38] D. Ti, H. Hao, C. Tong, J. Liu, L. Dong, J. Zheng, et al., LPS-preconditioned mesenchymal stromal cells modify macrophage polarization for resolution of chronic inflammation via exosome-shuttled let-7b, J. Transl. Med. 13 (1) (2015) 1–14.
[39] X. Ying, Q. Wu, X. Wu, Q. Zhu, X. Wang, L. Jiang, et al., Epithelial ovarian cancer-secreted exosomal miR-222-3p induces polarization of tumor-associated macrophages, Oncotarget [Internet] 7 (28) (2016) 43076–43087. Available from: http://www.oncotarget.com/fulltext/9246.
[40] G.R. Willis, A. Fernandez-Gonzalez, J. Anastas, S.H. Vitali, X. Liu, M. Ericsson, et al., Mesenchymal stromal cell exosomes ameliorate experimental bronchopulmonary dysplasia and restore lung function through macrophage immunomodulation, Am. J. Respir. Crit. Care Med. 197 (1) (2018) 104–116.
[41] Y.D. Jeon, K.S. Bang, M.K. Shin, J.H. Lee, Y.N. Chang, J.S. Jin, Regulatory effects of glycyrrhizae radix extract on DSS-induced ulcerative colitis, BMC Complement. Altern. Med. 16 (1) (2016) 4–13 [Internet]. Available from https://doi.org/10.1186/s12906-016-1390-8.
[42] J. Yao, J.Y. Wang, L. Liu, Y.X. Li, A.Y. Xun, Zeng W. Sen, et al., Anti-oxidant effects of resveratrol on mice with DSS-induced ulcerative colitis, Arch Med Res [Internet] 41 (4) (2010) 288–294. Available from: https://doi.org/10.1016/j.arcmed.2010.05.002.
[43] S. Vitale, C. Strisciuglio, L. Pisapia, E. Miele, P. Barba, A. Vitale, et al., Cytokine production profile in intestinal mucosa of paediatric inflammatory bowel disease, PLoS One 12 (8) (2017) 1–20.
[44] A.P.R. Paiotti, D.A. Ribeiro, R.M. Silva, P. Marchi, C.T.F. Oshima, R.A. Neto, et al., Effect of COX-2 inhibitor lumiracoxib and the TNF-α antagonist etanercept on TNBS-induced colitis in Wistar rats, J. Mol. Histol. 43 (3) (2012) 307–317.
[45] Y. Jin, Y. Lin, L. Lin, C. Zheng, *IL-17/IFN-γ* interactions regulate intestinal inflammation in TNBS-induced acute colitis, J. Interf. Cytokine Res. 32 (11) (2012) 548–556 [Internet]. Available from http://online.liebertpub.com/doi/abs/10.1089/jir.2012.0030.
[46] N.D. Zdravkovic, I.P. Jovanovic, G.D. Radosavljevic, A.N. Arsenijevic, N.D. Zdravkovic, S.L. Mitrovic, et al., Potential dual immunomodulatory role of VEGF in ulcerative colitis and colorectal carcinoma, Int. J. Med. Sci. 11 (9) (2014) 936–947.
[47] T. Kucharzik, R. Stoll, N. Lugering, W. Domschke, Circulating antiinflammatory cytokine IL-10 in patients with inflammatory bowel disease (IBD), Clin. Exp. Immunol. 100 (3) (1995) 452–456.
[48] J.O. Lindsay, C.J. Ciesielski, T. Scheinin, H.J. Hodgson, F.M. Brennan, The prevention and treatment of murine colitis using gene therapy with adenoviral vectors encoding IL-10, J. Immunol. 166 (12) (2001) 7625–7633 [Internet]. Available from: http://www.jimmunol.org.hsl-ezproxy.ucdenver.edu/content/166/12/7625%5Cnhttp://www.ncbi.nlm.nih.gov/pubmed/11390520.
[49] M. Lampinen, A. Waddell, R. Ahrens, M. Carlson, S.P. Hogan, $CD14^+$ $CD33^+$ myeloid cell-CCL11-eosinophil signature in ulcerative colitis, J Leukoc Biol [Internet] 94 (5) (2013) 1061–1070. Available from: http://doi.wiley.com/10.1189/jlb.1212640.
[50] M. Coskun, M. Salem, J. Pedersen, O.H. Nielsen, Involvement of JAK/STAT signaling in the pathogenesis of inflammatory bowel disease, Pharmacol. Res. 76 (2013) 1–8 [Internet]. Available from https://doi.org/10.1016/j.phrs.2013.06.007.
[51] S. Zundler, M. Neurath, Integrating immunologic signaling networks: the JAK/STAT pathway in colitis and colitis-associated cancer, Vaccines 4 (1) (2016) 5 [Internet]. Available from http://www.mdpi.com/2076-393X/4/1/5.
[52] W. Klein, A. Tromm, C. Folwaczny, M. Hagedorn, N. Duerig, J. Epplen, et al., The G2964A polymorphism of the STAT6 gene in inflammatory bowel disease, Dig. Liver Dis. 37 (3) (2005) 159–161.
[53] M.J. Rosen, M.R. Frey, M.K. Washington, R. Chaturvedi, L.A. Kuhnhein, P. Matta, et al., STAT6 activation in ulcerative colitis: a new target for prevention of IL-13-induced colon epithelial cell dysfunction, Inflamm. Bowel Dis. 17 (11) (2011) 2224–2234.
[54] C. Van Kampen, J. Gauldie, S.M. Collins, Proinflammatory properties of IL-4 in the intestinal microenvironment, Am J Physiol Liver Physiol 288 (1) (2005) G111–G117 [Internet]. Available from: http://www.physiology.org/doi/10.1152/ajpgi.00014.2004.
[55] J. Cosín-Roger, D. Ortiz-Masiá, S. Calatayud, C. Hernández, J.V. Esplugues, M.D. Barrachina, The activation of Wnt signaling by a STAT6-dependent macrophage phenotype promotes mucosal repair in murine IBD, Mucosal Immunol. 9 (4)

(2016) 986–998.
[56] Kisseleva T, Bhattacharya S, Braunstein J, Schindler CW. Signaling through the JAK/STAT pathway, recent advances and future challenges. Gene [Internet]. 2002;285:1–24. Available from: papers2://publication/uuid/52DB5F5A-0DED-4392-B708-CC00F109C47B.
[57] S. Schreiber, P. Rosenstiel, J. Hampe, S. Nikolaus, B. Groessner, A. Schottelius, et al., Activation of signal transducer and activator of transcription (STAT) 1 in human chronic inflammatory bowel disease, Gut 51 (3) (2002) 379–385 [Internet]. Available from http://ovidsp.ovid.com/ovidweb.cgi?T=JS&PAGE=reference&D=emed5&NEWS=N&AN=2002299551.
[58] S.K. Bandyopadhyay, C.A. De La Motte, S.P. Kessler, V.C. Hascall, D.R. Hill, S.A. Strong, Hyaluronan-mediated leukocyte adhesion and dextran sulfate sodium-induced colitis are attenuated in the absence of signal transducer and activator of transcription, Am. J. Pathol. 173 (5) (2008) 1361–1368 [Internet]. Available from: https://doi.org/10.2353/ajpath.2008.080444.
[59] R. Galien, D. Merciris, F.P. Vanhoutte, C. Delachaume, F.S. Namour, B. Vayssière, et al., 188 exploration of GLPG0634, the first selective JAK1 inhibitor, in inflammatory bowel disease is supported by early clinical results and mouse DSS-colitis data, Gastroenterology 146 (5) (2014) S–49 [Internet]. Available from https://linkinghub.elsevier.com/retrieve/pii/S0016508514601712.